Self-diffusion in networks of $CPClO_3$ wormlike micelles

N. Morié, W. Urbach, and D. Langevin
Laboratoire de Physique Statistique de l'Ecole Normale Supérieure 24 Rue Lhomond, 75231 Paris Cedex 05, France
(Received 21 March 1994)

We have studied self-diffusion in networks of cetylpyryidinium chlorate ($CPClO_3$) wormlike micelles by fluorescence recovery after fringe-pattern photobleaching techniques. Three different regimes are observed as we increase the surfactant. First, at low surfactant concentrations, the micelles are not entangled and the diffusion is fast. However, above the entanglement concentration, the diffusion coefficient decreases to a minimum value. Further increases in surfactant concentration beyond this minimum reveal a third stage in which the diffusion coefficient begins to increase. In addition to comparing our data to existing theories, we also develop a model that incorporates the special details related to our experimental technique. The analysis suggests that the micelles are partially interconnected, which is in agreement with the rheological behavior in these solutions.

PACS number(s): 36.20.−r, 05.40.+j, 51.20.+d, 82.70.−y

I. INTRODUCTION

Surfactant molecules in solution can self-assemble into a variety of different aggregates, such as spherical micelles, cylinders, or bilayers. Which type of aggregate depends on the molecular structure of the surfactant, interactions between the molecules, the nature of the solvent, and the surfactant concentration [1]. When salt is added to aqueous solutions of spherical micelles made with ionic surfactants, the electrostatic interactions between neighboring molecules are screened and the micelles elongate into cylindrical tubes. In fact, some ionic surfactants, such as cetyltrimethylammonium bromide (CTAB) or cetylpyridinium chlorate ($CPClO_3$), will produce very long and flexible cylinders, and when their concentration is high enough these cylinders entangle like polymer chains [2,3]. A similar behavior has also been observed with reverse micelles upon addition of small amounts of water [4].

The rheological behavior of systems with highly elongated cylindrical micelles is extremely interesting. In the entangled regime, the solutions are very viscous and eventually become elastic. However, the rheological behavior is more complex than for polymers. Because the micelles are not permanent aggregates, they break and recombine on time scales τ_{break} typically of milliseconds. Depending on the time scale t_{expt} of the experiment compared to τ_{break}, different aspects of the micelle behavior can be probed. If $t_{expt} < \tau_{break}$ as in light scattering experiments, cylindrical micelles behave like polymers, but when $t_{expt} > \tau_{break}$, the micelles have time to break and recombine, and their evolution is much different. Several theories have been developed to interpret the experiments in this second regime. One can assume that the relaxation of the rheological constraints involves, as for polymer chains, a reptation of the micelles in tubes formed by the other micelles. In this way, Cates [5] calculated the role of reversible scissions on the rheological properties. He also predicted the behavior of the diffusion coefficient D of a cylindrical micelle segment in this case. For polymers, the viscosity η is a power law of the polymer length and concentration. In the case of micelles, the length L of the micelle is not constant, but increases with the mass fraction ϕ. Current expectations lead to $L \sim \phi^{0.6}$ for entangled cylindrical micelles in the dilute regime [5]. It is then possible to predict that the viscosity η should scale as $\phi^{5.7}$ in the absence of scissions, and as ϕ^4 with the scissions. Similarly, the diffusion coefficient D is predicted to scale as ϕ^{-3} and $\phi^{-1.7}$, respectively [5].

Theoretical predictions are in good agreement with the rheological properties of CTAB solutions [2], as well as with the behavior of the diffusion coefficient at moderate salt concentrations [6]. At low salt concentrations there are discrepancies, which can be attributed to a more rapid growth of the micelles with concentration (i.e., $L \sim \phi^{\alpha}$ with $\alpha > 0.6$). Indeed, the micellar growth is due to the screening of the electrostatic interactions between the surfactant polar heads, and to a corresponding lowering of the spontaneous curvature of the aggregate when the ionic strength increases. The surfactant being ionic, an increase of ϕ corresponds to an increase of ionic strength, which can be significant if the salt concentration is comparable to or smaller than the surfactant concentration. Large salt concentrations produce a broad size distribution of the micelles, and anomalous diffusion is sometimes observed [7]. It is more difficult to interpret the data with $CPClO_3$ micelles which are very long, probably longer than CTAB micelles at an equivalent salinity, but which have relatively low viscosities [8,9]. It has been postulated that $CPClO_3$ micelles are partially interconnected [10].

Recently, Turner, Marques, and Cates [11] introduced additional relaxation mechanisms that account for bond interchange (two chains cross, form a four-armed star, and form two additional chains by exchanging the segments), end-end interchange (one chain forms a three-armed star by fusing with the end of another chain, and two additional chains are formed by exchanging the segments). These mechanisms were postulated to account

for the behavior of the micelles lifetime in the case of nonionic surfactants, or ionic surfactants at large ionic strength [12]. Turner, Marques, and Cates also analyzed the behavior of the solutions in another regime, $\tau_{break} < \tau_{Rouse}$, where τ_{Rouse} is the time scale for the breathing motion of the chain. Although τ_{Rouse} is very short, experimental situations of this kind might be encountered for very long micelles, such as those of the $CPClO_3$ system.

In the present paper, we will present diffusion coefficient measurements, where we have covered a wide salinity and surfactant concentration range. In particular we study the high micelle mass fraction range, where a change in the diffusion behavior is observed: D increases with ϕ. This is possibly due to the intrinsic motion of the probe in the method that we have used: fluorescence recovery after fringe-pattern photobleaching (FRAPP). In order to clarify the origin of the behavior at high ϕ, we have extended the predictions of the theory and obtained exponents for the different cases: reversible chain breaking, end-end interchange, and bond interchange. We have also studied the temperature dependence of D for different micelle mass fractions, which allows us to determine the corresponding activation energies.

II. THEORETICAL BACKGROUND

Cylindrical micelles longer than their persistence length l_p are similar to flexible polymers. If they are long enough to be entangled at low mass fraction they are in the semidilute regime. Moreover, in a good solvent for the micelles, each cylindrical micelle can be seen as a string of blobs of size ξ [13]. At length scales smaller than ξ the chain is swollen, with $\xi = l_p g^{\nu}$, where g is the number of persistence lengths within a blob, and ν is the excluded volume exponent: $\nu = 0.588$ ($\frac{3}{5}$ in the mean field approximation). Viewed at length scales larger than ξ, the solution is a homogeneous compact assembly of blobs. This homogeneity directly yields the scaling law for g by means of

$$\phi \sim \frac{g}{\xi^3} \sim g^{1-3\nu} . \tag{1}$$

In Eq. (1), as in all the following scaling laws, the persistence length is assumed to be independent of ϕ. This, as well as the whole preceding description, is supported by quasielastic light scattering measurements of $\xi_H(\phi)$, the screening length, which scales like ξ and was found [14] to vary like $\phi^{-0.75}$ for $CPClO_3$ with 1- and 0.1-M $NaClO_3$. The theoretical prediction from (1) is $\xi \sim \phi^{-0.77}$.

Theories which describe the dynamics of entangled polymers are based [13,15] on the assumption that any macromolecule can only move along a tube formed by the surrounding chains. In the semidilute regime the tube diameter is given by the blob size ξ, while the tube length in which a chain is confined is $L_T = (L/gl_p)\xi$, where L is the chain length. Chain diffusive motion proceeds through successive disengagements from this tube, which occur after curvilinear diffusion of the chain along its tube with a friction coefficient [12],

$$f = 6\pi\eta\xi \frac{L}{gl_p} ,$$

which is the friction coefficient for one blob times the number of blobs. The three-dimensional extension of the tube, R, is that of an ideal random walk of L/gl_p steps, each of length ξ, owing to the screening of the excluded volume interactions between blobs of the same chain by the other blobs,

$$R^2 = \xi^2 \frac{L}{gl_p} .$$

The duration of a full disentanglement by curvilinear diffusion (reptation) in the tube is

$$\tau_{rep} = D_c^{-1} \left[\frac{L}{l_p g} \right]^2 \xi^2 ,$$

with a curvilinear diffusion coefficient

$$D_c = \frac{kT}{f} = \frac{kT}{6\pi\eta\xi} \left[\frac{L}{gl_p} \right]^{-1} .$$

The macroscopic diffusion coefficient D, for successive jumps of length R every τ_{rep} is

$$D_{rep} = \frac{R^2}{\tau_{rep}} = \frac{kT}{6\pi\eta\xi} \left[\frac{L}{gl_p} \right]^{-2} . \tag{2}$$

D_{rep} describes the center of mass diffusion of a chain for times which are long compared to τ_{rep}. Its derivation neglects the tube length fluctuations, which develop on a time scale $t < \tau_{Rouse} = \tau_{rep}(gl_p/L)$. For $t < \tau_{Rouse}$, the main contribution to the displacement of a monomer of the chain, or of a probe attached to it, comes from the tube length fluctuations rather than from the curvilinear diffusion of the whole chain [13,15].

To sum up, at $t < \tau_{Rouse}$ a monomer diffuses along the tube by means of tube length fluctuations until, after τ_{Rouse}, the maximum amplitude of the fluctuation is reached. Then for $\tau_{rep} > t > \tau_{Rouse}$ the monomer diffuses by curvilinear diffusion along the tube, and for $t > \tau_{rep}$ the monomer experiences a three-dimensional Brownian motion with a diffusion coefficient given by (2).

This picture has to be modified in two respects when one studies giant cylindical micelles with FRAPP.

The first modification comes from the finite lifetime τ_{break} of a micelle. If $\tau_{break} < \tau_{rep}$, the elementary step of the Brownian motion (i.e., the disengagement of a whole micelle from its tube of constraints) is interrupted by a transfer of mass with other micelles before its completion. Furthermore, it is no longer possible to define a diffusion coefficient for a micelle on time scales greater than τ_{break}. In order to describe the diffusion of the surfactant molecules, one must follow the movement of smaller segments of micelles whose length is so defined that their integrity is preserved during each of the elementary independent steps of their Brownian motion. Such a segment of micelle has a constant curvilinear coordinate along the micelle during its lifetime τ_{break} and will thus be called, in analogy with polymers, a monomer.

A new elementary step is defined where τ is its duration and l_t the tube length explored. If on average one transfer of mass occurs within the tube length l_t in the time τ necessary for this exploration, then successive jumps (τ, l_t) are at least partially uncorrelated. They verify the set of equations

$$\tau = \frac{L\xi}{l_t l_p g}\tau_{\text{break}} , \tag{3a}$$

$$l_t^2 = f(\tau) , \tag{3b}$$

where $f(\tau)$ depends on the dominant mechanism of diffusion on time scale τ, either reptation,

$$f(\tau) = D_c\tau , \tag{4a}$$

or breathing [15],

$$f(\tau) = D_c\left[\frac{\tau}{\tau_{\text{Rouse}}}\right]^{-1/2}\tau = \frac{L\xi^2\left[\frac{\tau}{\tau_{\text{Rouse}}}\right]^{1/2}}{gl_p} . \tag{4b}$$

The three-dimensional diffusion coefficient is then

$$D = l_t\xi\tau^{-1} . \tag{5}$$

Equation (3a) defines the lifetime of a segment of tube of length l_t, assuming that the probability of mass transfer is uniform along the micelle.

In FRAPP experiments we measure the diffusion of a probe which is free to move along the micelle. In the previous analysis in terms of monomer diffusion, the probes are held fixed with respect to the micelles. This analysis is only valid as far as the probe diffusion relative to the micelle can be ignored. In the other limit, if the probe is allowed to diffuse along the micelles and the curvilinear deplacement of the micelles is neglected, two regimes may arise. In the first one, the probe only explores a portion of the micelle length before a transfer of mass occurs within the already explored length. This diffusion is described by Eqs. (3a) and (5). Equation (3b) gives l_t, the tube length explored by the probe in time τ:

$$l^2 = D_S\tau ,$$

with l the micellar length explored in time τ:

$$l_t = \xi\frac{l}{gl_p} ,$$

$$l_t^2 = \frac{D_S\tau\xi^2}{(gl_p)^2} ,$$

where D_S is the diffusion coefficient of the probe along the micelle. We will call this regime free. In the second regime the probe is assumed to have explored the whole micelle in less than its lifetime, and then waits for a transfer of mass to happen in order to diffuse further. The probe makes jumps of length $\xi(L/gl_p)^{1/2}$, every τ_{break}, which yields a diffusion coefficient D_{wait}:

$$D_{\text{wait}} = \left[\frac{L}{gl_p}\right]\frac{\xi^2}{\tau_{\text{break}}} ,$$

which can be written in terms of D_{rep} [Eq. (2)]:

$$D_{\text{wait}} = D_{\text{rep}}\frac{\tau_{\text{rep}}}{\tau_{\text{break}}} . \tag{6}$$

In order to derive scaling laws for each mode of diffusion, we need the ϕ dependence of τ_{break}, the lifetime of a micelle. Following the analysis of Ref. [11], three kinetics of mass transfer will be distinguished:

$$\begin{aligned} &\text{reversible scission,} && \tau_{\text{break}} = (kL)^{-1} \\ &\text{end interchange,} && \tau_{\text{break}} = (k\phi)^{-1} \\ &\text{bond interchange,} && \tau_{\text{break}} = (kL\phi)^{-1} , \end{aligned} \tag{7}$$

where L is the average micellar length, ϕ is the surfactant mass fraction, and k is a reaction rate. The scaling laws for the diffusion coefficient are summed up in Table I, where the dependence of the average micellar length L on ϕ is not explicit.

TABLE I. Expressions of the self-diffusion coefficient for different kinetics of mass transfer between micelles, and different ratios $\tau_{\text{rep}}/\tau_{\text{break}}$. L is the average micellar length, k is a kinetic constant, D_S is the self-diffusion coefficient of the probe along a micelle, and ϕ is the surfactant mass fraction.

	$\tau_{\text{break}} < \tau_{\text{rep}}$				$\tau_{\text{break}} > \tau_{\text{rep}}$
	Monomer diffusion		Probe diffusion		Micelle diffusion
Model	$D_{\text{breathing}}$ Eq. (4b)	$D_{\text{reptation}}$ Eq. (4a)	D_{wait}	D_{free}	$D_{\text{reptation}}$
Reversible scission	$k^{3/5}\phi^{-1.4}$	$k^{1/3}\phi^{-1.3}L^{-2/3}$	$k\phi^{-0.2}L^2$	$D_S^{2/3}K^{1/3}\phi^{-0.2}$	
End interchange	$k^{3/5}\phi^{-0.8}L^{-3/5}$	$k^{1/3}\phi^{-1.0}L^{-1}$	$k\phi^{+0.8}L^1$	$D_S^{2/3}k^{1/3}\phi^{0.1}L^{-1/3}$	$L^{-2}\phi^{-1.85}$
Bond interchange	$k^{3/5}\phi^{-0.8}$	$k^{1/3}\phi^{-1.0}L^{-2/3}$	$k\phi^{+0.8}L^2$	$D_S^{2/3}k^{1/3}\phi^{0.1}$	

III. EXPERIMENTAL METHODS AND RESULTS

Fluorescence recovery after fringe-pattern photobleaching (FRAPP) experiments allow the measurement of the self-diffusion coefficient D of fluorescent probes embedded in the micelles [6,18]. When strongly illuminated, these probes loose their fluorescence properties (photobleaching). The time evolution of the fluorescence intensity of the illuminated volume is measured afterwards using a low intensity light beam. The signal increases as unbleached probes enter the studied volume, and D is deduced from its recovery time. The beam diameter is about 1 mm. The bleaching pulse duration is 20 or 50 ms, the bleaching power in the sample is about 500 mW. The fluorescence recovery is monitored with a beam of intensity about 10^4 times lower than the bleaching power. The recovery curves are well fitted by a single exponential function: $f(t)=A\exp(-t/\tau)+B$, where $\tau=i^2/4\pi^2D$; i is the fringe spacing (20 to 100 μm), and D is the self-diffusion coefficient. For each sample we checked that the recovery time scaled as i^2, and D was deduced from a linear fit of τ vs i^2.

This study was performed with $CPClO_3$ in brine. The salt was $NaClO_3$. The $CPClO_3$ was a generous gift [17], and the $NaClO_3$ was from Merck. Four series of solutions with different salinities were prepared, at 1, 0.1, and 0.05 M and without brine. For each salinity the $CPClO_3$ mass fraction was varied from 10^{-4} to 0.3. All the experiments were performed at 35°C(±0.1°C). The probe molecules are also surfactant molecules, the polar head is a fluorescein group, and the apolar part is a carbon chain. In order to check the possible influence on the diffusion coefficient of exchanges of the probe between the micelles and the solvent, we have used probes with different carbon chains [16]. For a given solution, the same diffusion coefficient was measured irrespective of the aliphatic chain length of the probe, whereas the ratio of the probes resisdence times in the solvent is of the order 1000 [18] when the chain length is increased from 12 to 18 carbons. Thus the time spent by the probe in the solvent has no overall effect on the measured diffusion coefficient. In order to prevent an alteration of the micellar phase by the addition of probe molecules, the mass ratio of probe to surfactant was always kept at less than 0.5%.

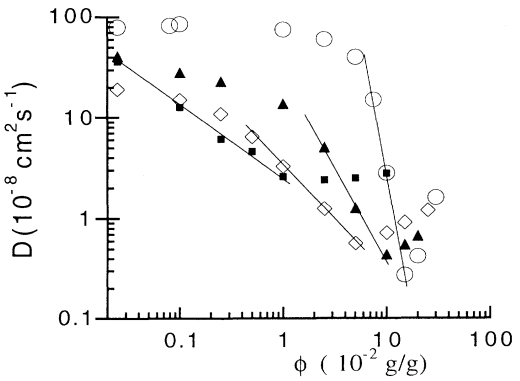

FIG. 1. Log-log plot of the self-diffusion coefficient vs surfactant concentration. The values of the slopes are −5.5 for 0 M (open circles), −1.7 for 0.05 M (triangles), −1.0 for 0.1 M (diamonds), and −0.75 for 1 M (squares).

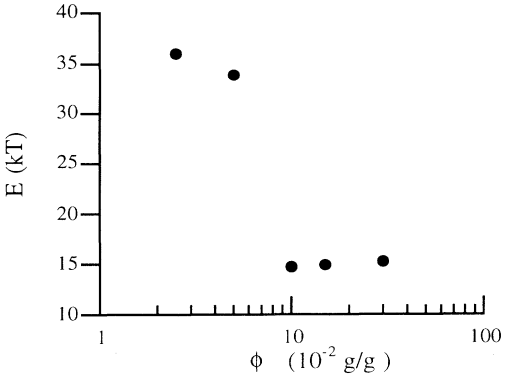

FIG. 2. Dependence of the activation energies in $D\sim\exp(-E/kT)$ on the surfactant mass fraction, for solutions of $CPClO_3$ with 0.1 M of $NaClO_3$.

The results for all the samples are gathered in Fig. 1, where we have plotted the values of the self-diffusion coefficient D versus the surfactant concentration on a log-log scale. For salinities lower than 1 M we have a plateau or a slight decrease of D up to a certain mass fraction ϕ^* and then a sharp decrease up to a certain values ϕ^{**}, followed by an increase of D values. When enough salt is added (1 M) only the two last regimes are observed. The experimental errors correspond approximately to the size of the points.

The variation of D with temperature was measured for solutions at 0.1-M $NaClO_3$ concentration. D follows an Arrhenius law, and $D(\phi)\sim\exp[-E(\phi)/kT]$. The values of $E(\phi)$, in units of kT, are shown as a function of ϕ, the surfactant mass fraction, in Fig. 2.

IV. DISCUSSION

A. Dilute regime, $\phi<\phi^*$

When no salt is added, the self-diffusion coefficient remains independent of the surfactant concentration up to $\phi=5\times10^{-3}$ g/g, and $D=8.10^{-7}$ cm^2/s. Assuming that the micelles are spherical, and using $D=kT/(6\pi\eta R)$, we obtain $R\sim25$ Å, consistent with the radius of $CPClO_3$ cylindrical micelles measured by neutron scattering at high salinities, 1 and 0.1 M [14]. For 0.05- and 0.1-M salt, D decreases slowly, the micelles are not yet entangled, and their length probably starts to increase slightly.

B. Semidilute regime

Above ϕ^*, D experiences a fast decrease, following a power law: $\phi^{-\delta}$. δ is 5.5, 1.7, 1, and 0.75, respectively, in 0-, 0.05-, 0.1-, and 1-M brine. This sensitivity to brine concentration has already been noticed for CTAB [6], and has been ascribed to the modification of the growth

law of the micelles and the part played by counterions at low brine concentration [19]. For a given salinity and in a similar concentration range, the exponent δ is much smaller for CTAB than for $CPClO_3$ micelles: 4.4, 2, and 1.4 for 0.05-, 0.1-, and 0.25-M salt, respectively. Since the surfactant concentration ranges are similar in both cases, one is led to the conclusion that the electrostatics is different in the two cases. This is possibility associated with a more rapid counterion condensation in the $CPClO_3$ systems, also explaining the much more rapid micellar growth in these systems.

For CTAB, the limit value of δ at moderate salt concentration is compatible with Cates' prediction of reptation with chain breakage and recombination. For $CPClO_3$, the high salt values of δ are clearly smaller. However, as for CTAB samples we observe a single exponential behavior of the recovery curves. This means that the chain breakage and recombination occurs at characteristic times smaller than the experimental time (i.e., $t_{expt} > \tau_{rep} > \tau_{break}$ or $t_{expt} > \tau_{break} > \tau_{rep}$). In the case of CTAB, which follows Cate's model, $t_{expt} > \tau_{rep} > \tau_{break}$.

For low salt concentrations ($c < 0.1$ M) the electrostatic interactions are probably not fully screened. In that case the micelles' average length and the kinetic of the mass transfer dependence on ϕ due to the addition of surfactant ions are difficult to model, and there is no quantitative theory for $k(\phi)$ or $L(\phi)$. We will come back to this case below, in connection with the discussion of the concentrated regime.

When more salt is added, the ϕ dependence of the micellar length L will be assumed to be $L = \phi^{\alpha}$ with $\alpha = 0.6$ [4], as for nonionic surfactants. The kinetic constant of the reaction of mass transfer should be ϕ independent as long as the surfactant concentration remains small compared to the brine concentration; in this way the surfactant ions do not change the total ionic strength. In Table II we showed the results for the monomer diffusion coefficient within this approximation. Also shown in Table II are the predictions for the viscosity according to Ref. [11]. In this table it is clearly seen that exponents compatible with the experiments correspond to the smallest ones. In particular, the experiments suggest that the relaxation observed are in the breathing regime. For 1-M salt, the data are consistent with the bond-interchange mechanism, whereas for 0.1-M salt they are closer to an end-interchange-driven process. Our results suggest that these micelles do not reptate in the semidilute regime. At 1-M salt the micelles are very long since they are entangled at concentrations as low as 10^{-3} g/g [9]. The blob size has been estimated at roughly 2.10^3 Å at this concentration [20], which yields a diffusion coefficient for a blob already smaller than the measured value of 10^{-7} cm^2 s^{-1}, not to speak of the diffusion coefficient of a reptating string of such blobs.

TABLE II. Different dynamical regimes for the viscosity and the monomer self-diffusion coefficient, according to Ref. [12], when the growth law of the micelles is supposed to be of the form $L \sim \phi^{-0.6}$, where ϕ is the surfactant mass fraction.

Model	Coefficient	Regime		
		Unbreakable chains	Reptative	Breathing
Bond interchange	η	$\phi^{5.7}$	$\phi^{4.0}$	$\phi^{2.6}$
	D	$\phi^{-3.0}$	$\phi^{-1.4}$	$\phi^{-0.8}$
Reversible scission	η	$\phi^{5.7}$	$\phi^{3.7}$	$\phi^{3.2}$
	D	$\phi^{-3.0}$	$\phi^{-1.7}$	$\phi^{-1.4}$
End interchange	η	$\phi^{5.7}$	$\phi^{3.5}$	$\phi^{2.9}$
	D	$\phi^{-3.0}$	$\phi^{-1.6}$	$\phi^{-1.2}$

Unfortunately, the results for the bulk viscosity of the same systems cannot be accounted for by the theory, even in the breathing regime as for the diffusion coefficient, the viscosity scales as $\eta \sim \phi^{\beta}$, with $\beta = 2$ and 1 for 0.1- and 1-M salt, respectively [11]. The discrepancy is especially large for 1-M salt. It is possible that the scission and other processes described above are affected by shear stresses.

C. Concentrated regime

Above ϕ^{**}, D increases like $\phi^{\delta'}$. Rough estimates of δ' values lead to 1.5, 1, 0.6, and 0, respectively, for 0-, 0.05-, and 0.1-, and 1-M brine. It is associated with a change of activation energy (Fig. 2). However, hereafter we will only discuss the behavior of δ', because the activation energies cannot be accounted for in the present state of the theories. This change of behavior can either come from a modification of the micellar structure, or it can reflect a change of the mechanism of probe diffusion in an unaltered system.

1. Disconnected micelles

Assuming that the micellar structure is not altered, in particular that the micelles remain disconnected, the models discussed so far in Table II, in which the fluorescent probe diffuses solidarily with the micelle (i.e., monomer diffusion) are still valid, but they all give positive δ values as long as L increases with ϕ and k is not too strongly dependent on ϕ. If the fluorescent probe is allowed to diffuse by a mechanism no longer identical to the one followed by the monomers, the probe diffusion, which is measured in FRAPP, can become an increasing function of ϕ, while the monomer diffusion remains a decreasing function of ϕ. This would also explain why the rheological properties of the solution, which are concerned with the dynamics of monomers, do not seem to be affected when ϕ^{**} is crossed [9].

An obvious way to modify the probe diffusion would be to allow the probe to pass from one micelle to an other by the mere contact of two micelles, not involving any of the mass transfers described above [Eq. (7)]. As the surfactant concentration increases, so does the frequency of contacts between micelles, allowing for an increase in D. This kind of flip-flop motion of the probe at a contact point between two micelles involves an energy barrier which should depend on the aliphatic tail of the probe. A probe with a short tail will pass more easily from one micelle to the other than a large one, and thus diffuse more quickly. This does not appear to be the case: we did not

see any change in D larger than our typical experimental errors, when the tail length of the fluorescent probe was increased from 12 to 18 carbons and when a single chain was replaced by a double chain [16].

The assumption that the probe diffuses like a monomer can also break down when the diffusion of the probe along the micelle is faster than the curvilinear motion of the micelle itself in its tube. This could occur at high surfactant concentration when the micelle motion slows down. In these regimes of probe diffusion, one can see from Table I that only $D_{wait}(\phi)$, which increases significantly with ϕ and/or $L(\phi)$, is able to describe the sudden increase of $D(\phi)$ for $\phi > \phi^{**}$.

In this picture, the concentration ϕ^{**} has a precise physical meaning. It is the concentration at which $D_{mono} = D_{wait}$: the diffusion of the probe overtakes the diffusion of a monomer. Two cases must be distinguished according to the mode of monomer diffusion when $\phi < \phi^{**}$ (i.e., in the semidilute regime):

(i) If $\tau_{break} > \tau_{rep}$ when $\phi < \phi^{**}$, one should observe a diffusion by pure reptation before the crossover: $D_{mono} = D_{rep}$. Thus at $\phi = \phi^{**}$ we have $D_{wait} = D_{rep}$ and also $\tau_{break} = \tau_{rep}$ from Eq. (6). For $\phi > \phi^{**}$, we have

$$D_{wait} = D_{rep}\tau_{rep}/\tau_{break} > D_{rep} ,$$

assuming that the micellar length increases with ϕ, and thus that τ_{rep}/τ_{break} increases with ϕ. The case where $\tau_{Rouse} < \tau_{break} < \tau_{rep}$, when $\phi < \phi^{**}$, cannot occur, because the diffusion of the monomer is then always slower than D_{wait}. This is readily seen if the two diffusion coefficients are expressed in terms of D_{rep} from Eq. (6) for D_{wait} and Eqs. (3), (4a), and (5) for D_{mono};

$$D_{wait} = D_{rep}\tau_{rep}/\tau_{break}$$

and

$$D_{mono} = D_{rep}(\tau_{rep}/\tau_{break})^{1/3} ,$$

in other words, $D_{wait} > D_{mono}$ as long as $\tau_{rep} > \tau_{break} > \tau_{Rouse}$. So D_{wait} is observed as soon as $\tau_{rep} > \tau_{break}$. For any concentration $\phi < \phi^{**}$, the diffusion is then a pure reptation given by $D_{rep} = L^{-2}\phi^{-1.85}$. For any growth low of $L(\phi)$, it gives, for $\phi < \phi^{**}$, a value of $\delta > 1.85$. However, this is not compatible with the observed values at 0.1- and 0.05-M brine, which are $\delta = 1$ and 1.7, respectively.

(ii) The other possible combination of monomer diffusion for $\phi < \phi^{**}$, followed by D_{wait} for $\phi > \phi^{**}$, happens if $\tau_{break} < \tau_{Rouse}$ for $\phi < \phi^{**}$. The value of δ could then be as low as 0.8 if the monomers diffuse by tube length fluctuations associated with a bond interchange kinetic of mass transfer (see Table I). However, in this case D is independent of $L(\phi)$. In order to obtain an L dependent diffusion coefficient, which could account for the variations of δ at low brine contractions, the end-interchange kinetic model is required.

In conclusion, if the increase of D for $\phi > \phi^{**}$ were due to the diffusion of the probe D_{wait}, there could be two different mechanisms of monomer diffusion for $\phi < \phi^{**}$: pure reptation or Rouse motion. We have seen that pure reptation alone cannot account for the small δ values observed at high brine concentration. If pure reptation describes the diffusion at low brine concentration and for $\phi < \phi^{**}$, there must be, as brine is added, a transition from pure reptation to Rouse motion. However, this transition is very unlikely. It requires a jump of τ_{break} from τ_{rep} to τ_{Rouse} because intermediate values of τ_{break} are not compatible with the observation of D_{wait}. On the other hand, a diffusion by Rouse motion can describe the diffusion for $\phi < \phi^{**}$ and for all salinities. In order to account for the δ values, it requires a transition from an end-interchange kinetic to a bond-interchange kinetic as brine is added. This seems to be the only combination of models from Table I which describes our data coherently.

The results for $CPClO_3$ are thus consistent with $\tau_{break} < \tau_{Rouse}$, whereas those for CTAB which correspond to reptation steps interrupted by breakages are consistent with $\tau_{rep} > \tau_{break} > \tau_{Rouse}$. This fact suggests that τ_{break} is much shorter for $CPClO_3$ micelles than for CTAB ones at a given salinity.

2. *Connected micelles*

The increase in D at high ϕ can also be a consequence of an alteration of the micellar structure. The viscosity data are compatible with the existence of connections, as soon as the micelles are entangled, i.e., above ϕ^*. The diffusion coefficient measurement suggest that the role of the connections is negligible before ϕ^{**}. One way to reconcile the two pictures is to assume that the ratio C of connections over entanglements is very small, and that during the diffusion motion below ϕ^{**} the distance traveled by the probe during τ_{break} is smaller than the distance between two connections. Even if C remains constant, the density of entanglements increases when ϕ increases, so above ϕ^{**} the connections might start to play a role on the diffusion process.

CTAB micelles have comparable diffusion coefficients, but do not show a D increase at large ϕ. Rather D saturates to a constant value above ϕ^{**} [21]. The behavior below ϕ^{**} can be described by monomer diffusion, and above ϕ^{**} by free diffusion (see Table I). This is compatible with rheological behavior, suggesting the absence of connections.

V. CONCLUSION

We have shown that at high and low salt concentrations, the self-diffusion of a fluorescent probe in solutions of $CPClO_3$ cylindrical micelles in the semidilute regime can be accounted for qualititavely if we assume that the cylindrical micelles form an unconnected entangled network and that the relaxation process is a Rouse motion. However, these assumptions are not fully compatible with the viscosity data.

Another hypothesis is that micellar branching occurs. This conclusion was previously reached by the authors of Ref. [12] mainly on the ground of the rheological properties of the solutions. In order to examine this hypothesis in detail by means of self-diffusion studies, a better theoretical understanding of the diffusion of a probe on a branched network is required.

ACKNOWLEDGMENTS

We are grateful to J. Appell and G. Porte for the gift of $CPClO_3$ and for many useful discussions. We also thank R. Zana for extremely useful comments. The Laboratoire de Physique Statistique de l'Ecole Normale Supérieure is Unité associée au Centre National de la Recherche Scientifique and associated with Universités Paris 6 and 7.

[1] J. Israelachvili, D. J. Mitchell, and B. W. Ninham, J. Chem. Soc. Faraday Trans. II **72**, 1525 (1976).

[2] S. J. Candau, E. Hirsch, and R. Zana, J. Phys. **45**, 1263 (1984); M. E. Cates and S. J. Candau, J. Phys. Condens. Matter **2**, 6869 (1990).

[3] H. Rehage and H. Hoffmann, J. Phys. Chem. **92**, 4712 (1988).

[4] P. Schurtenberger, R. Scartazzini, L. J. Magid, M. E. Leser, and P. L. Luisi, J. Phys. Chem. **94**, 3695 (1990).

[5] M. E. Cates, J. Phys. (Paris) **49**, 1593 (1988).

[6] R. Messager, A. Ott, D. Chatenay, W. Urbach, and D. Langevin, Phys. Rev. Lett. **60**, 1410 (1988).

[7] J. P. Bouchaud, A. Ott, D. Langevin, and W. Urbach, J. Phys. II **1**, 1465 (1991).

[8] J. Appell, G. Porte, A. Khatory, F. Kern, and S. J. Candau, J. Phys. II France **2**, 1045 (1992).

[9] A. Khatory, F. Kern, F. Lequeux, J. Appell, G. Porte, N. Morie, A. Ott, and W. Urbach, Langmuir **9**, 933 (1993).

[10] F. Lequeux, J. Phys. II **1**, 195 (1991).

[11] M. S. Turner, C. Marques, and M. E. Cates, Langmuir **9**, 693 (1993).

[12] R. Zana, in *Surfactants in Solutions,* edited by K. L. Mittal and P. Bothorel (Plenum, New York, 1986), Vol. 4, p. 115.

[13] P. G. de Gennes, *Scaling Concepts in Polymer Physics* (Cornell University press, Ithaca, NY, 1979); J. Chem. Phys. **76**, 3325 (1982).

[14] J. Appell and J. Marignan, J. Phys. II France. **1**, 1447 (1991).

[15] M. Doi and S. F. Edwards, *The Theory of Polymer Dynamics* (Clarendon, Oxford, 1986).

[16] The fluorescent probe references from Molecular Probes, Inc. (Eugene, OR 97402) are the following. (i) Single chain probes: *D*-109, *H*-110, and *O*-322 (12, 16, and 18 carbon atoms, respectively). (ii) Double chain probe: *F*-362 (2×16 carbon atoms). Data in Fig. 1 were obtained with *H*-110. The definitions of these materials are D-109: 5-(N-dodecanoyl)aminofluorescein. H-110: 5-(N-hexadecanoyl)aminofluorescein. O-322: 5-(N-octadecanoyl)aminofluorescein. F-362: N-(5-fluoresceinthiocarbamyl)-1,2-dihexadecanoyl-sn-glycero-3-phoshaothanolamino,triothylaminonium salt. (fluorescein DHPE).

[17] J. Appell and G. Porte, GDPC Université de Montpelier II, France.

[18] D. Axelrod, D. Koppel, J. Schlessinger, E. Elson, and W. Webb, Biophys. J. **16**, 1055 (1976). J. Davoust, P. F. Devaux, and L. Leger, Embo. J. **1**, 1233 (1982).

[19] S. A. Safran, P. A. Pincus, M. E. Cates, and F. C. MacKintosh, J. Phys. France **51**, 503 (1990).

[20] J. Appell and G. Porte, Prog. Colloid Polym. **84**, 41 (1991).

[21] A. Ott, N. Morié, W. Urbach, J. P. Bouchaud, and D. Langevin, J. Phys. IV **3**, 91 (1993).